Continuous-Time Random Walk for a Particle in a Periodic Potential

Andreas Dechant,[1] Farina Kindermann,[2] Artur Widera,[2,3] and Eric Lutz[4]
[1]WPI-Advanced Institute for Materials Research (WPI-AIMR), Tohoku University, Sendai 980-8577, Japan
[2]Department of Physics and Research Center OPTIMAS, University of Kaiserslautern, 67663 Kaiserslautern, Germany
[3]Graduate School Materials Science in Mainz, 67663 Kaiserslautern, Germany
[4]Institute for Theoretical Physics I, University of Stuttgart, 70550 Stuttgart, Germany

(Received 28 January 2019; revised manuscript received 4 April 2019; published 13 August 2019)

Continuous-time random walks offer powerful coarse-grained descriptions of transport processes. We here microscopically derive such a model for a Brownian particle diffusing in a deep periodic potential. We determine both the waiting-time and the jump-length distributions in terms of the parameters of the system, from which we analytically deduce the non-Gaussian characteristic function. We apply this continuous-time random walk model to characterize the underdamped diffusion of single cesium atoms in a one-dimensional optical lattice. We observe excellent agreement between experimental and theoretical characteristic functions, without any free parameter.

DOI: 10.1103/PhysRevLett.123.070602

Coarse graining is an essential tool for the study of complex systems. Different levels of description of a system's state are commonly identified [1,2]. The microscopic (fine-grained) level corresponds to the true mechanical state. Its complete characterization is often out of reach, both theoretically and experimentally, owing to its complexity. By contrast, the macroscopic (coarse-grained) regime consists of a few pertinent and accessible variables that capture the main features of the system. All irrelevant degrees of freedom are eliminated during coarse graining, for instance, by averaging over them. These various representations are usually associated with different time scales. Each of those may be used to define intermediate (mesoscopic) levels of coarse graining [1,2]. Equilibrium thermodynamics is a prominent example of a coarse-grained theory where averaged quantities such as volume, pressure, and temperature, are introduced to specify the macroscopic state [3,4]. On the other hand, far from thermal equilibrium, the coarse-graining method is more involved as the time evolution of the system needs to be accounted for [1–5]. Connecting fine-grained and coarse-grained descriptions is in general very challenging for any realistic nonequilibrium system [1–5].

Continuous-time random walks (CTRWs) are a well-established approach used to investigate the coarse-grained nonequilibrium dynamics of complex systems [6,7]. While jumps occur at fixed discrete times in standard random walks, they happen at random continuous times in a CTRW. Continuous-time random walks provide general models for normal as well as anomalous diffusion and transport processes. They are completely characterized by a jump-length distribution and a waiting-time distribution between two jumps. They offer an effective method to compute the probability distribution of the position of the random walker from which various transport properties, such as moments and correlation functions, may be determined. Continuous-time random walks have been successfully applied in a wide range of areas, ranging from disordered systems, plasmas and chaotic dynamics to turbulence, biology, and finance [8–12]. Experimental evidence for CTRWs has been found for microbead motion in reconstituted actin networks [13], lipid granules in cellular cytoplasm [14], protein channels in plasma membranes [15], and intermittent quantum dots [16]. A few microscopic derivations of CTRWs have been presented [17,18]. However, in most cases, continuous-time random walks are phenomenological as the complex microscopic dynamics is unknown.

In this Letter, we theoretically derive a CTRW model for a Brownian particle in a deep periodic potential starting from the microscopic level and directly compare its predictions to experiment. This system is ubiquitous in physics, chemistry, and biology [19,20]. The microscopic description is based on the Langevin equation, a stochastic extension of Newton's equation of motion [19,20]. This dynamics is not exactly solvable owing to the nonlinearity of the potential. The coarse-grained evolution is diffusive on very long time scales with a Gaussian probability distribution. Diffusion coefficients are known in terms of the microscopic parameters both in the underdamped and overdamped regimes [19–21]. However, no analytical results are available for the probability density or the position correlation function at intermediate finite times, despite their experimental importance [22,23]. A mesoscopic description is therefore needed. Such a model should be simpler than the microscopic Langevin equation to allow an analytical description of the statistics of the process and, at the same time, more detailed than the macroscopic Gaussian diffusion approximation.

In the following, we express the jump-length and the waiting-time distributions in terms of microscopic variables of the system. From these two distributions, we determine the Fourier-Laplace transform of the probability density, also known as the dynamical structure factor [8–12], as well as the characteristic function with the help of the Montroll-Weiss formula for uncorrelated CTRWs [24]. We use the characteristic function to derive explicit expressions for the lower moments and the position correlation function of the particle. We furthermore apply our theoretical results to describe the underdamped diffusion of single Doppler-cooled cesium atoms in a 1D optical lattice [25–27]. We obtain very good agreement between experiment and theory for the non-Gaussian characteristic function, both as a function of time and wave vector, without any free parameter. Finally, we determine the range of validity of the coarse-grained CTRW model from the experimental data and observe the transition to the macroscopic Gaussian diffusion approximation.

Continuous-time random walk model.—The continuous-time random walk extends the concept of a random walker, which randomly takes unit steps to the left or to the right at discrete time intervals, to a continuous process with arbitrary step sizes. The main ingredients of the CTRWs are the jump-length distribution $\phi(\xi)$ and the waiting-time distribution $\psi(\tau)$. When these distributions are mutually independent and the same for each step, they define a renewal process [6,7]. In that case, the probability distribution $P(x,t)$ is simply related to the waiting-time and jump-length distributions in Fourier-Laplace space through the Montroll-Weiss formula [24],

$$S(k,s) = \frac{1-\tilde{\psi}(s)}{s[1-\hat{\phi}(k)\tilde{\psi}(s)]}. \tag{1}$$

The dynamical structure factor $S(k,s)$ is here the Fourier-Laplace transform of $P(x,t)$, and $\hat{\phi}(k)$ and $\tilde{\psi}(s)$ are the respective Fourier and Laplace transforms of the jump-length and waiting-time distributions. Equation (1) fully characterizes the statistics of the CTRW at arbitrary times for given distributions $\phi(\xi)$ and $\psi(\tau)$. The latter are often determined phenomenologically. We will next explicitly derive both distributions for a Brownian particle moving in a periodic potential.

Let us consider a classical particle of mass m in contact with a heat bath at temperature T moving in a periodic potential, $U(x+L) = U(x)$, of period L and depth U_0. Its microscopic dynamics is governed by the underdamped Langevin equation for the velocity $v(t)$ [19,20],

$$\dot{v}(t) = -\gamma v(t) - \frac{1}{m}U'(x(t)) + \frac{\sqrt{2\gamma k_B T}}{m}\eta(t), \tag{2}$$

where $\eta(t)$ denotes a centered and delta-correlated Gaussian white noise, $\langle \eta(t)\eta(t')\rangle = \delta(t-t')$, γ is the damping coefficient, and k_B the Boltzmann constant. In order to cast the dynamics described by Eq. (2) in terms of a CTRW, we need to coarse grain and decompose it into a series of consecutive jump and waiting events. This can be done for deep potentials, $U_0 \gtrsim 4k_BT$, where the particle spends most of the time close to one of the minima of the potential and only occasionally escapes to another well [28]. We identify these trapping periods with the waiting times and the escape events with the jumps of the CTRW. In this limit of well-separated time scales, the escape process may be described by Kramers' rate theory, which states that the fraction of initially trapped particles remaining in a potential well decays over time at a rate $1/\tau_0$ [29]. This immediately translates into an exponential distribution for the escape times,

$$\psi(\tau) = \frac{1}{\tau_0}e^{-\tau/\tau_0}. \tag{3}$$

Performing the Laplace inversion of the dynamical structure factor [Eq. (1)], we thus obtain the characteristic function $K(k,t)$ in the time domain,

$$K(k,t) = e^{-(t/\tau_0)[1-\hat{\phi}(k)]}. \tag{4}$$

Compared to the probability distribution $P(x,t)$, this representation has two advantages: First, the dependence on the wave vector k for fixed time is simply related to the Fourier transform $\hat{\phi}(k)$ of the jump-length distribution. Second, at fixed k, the decay of the characteristic function is explicitly exponential in time, allowing us to easily verify the validity of Eq. (3) for a given jump process.

For a standard cosine-shaped potential, $U(x) = U_0[1-\cos(2\pi x/L)]/2$, the escape time τ_0 can be estimated both in the strong damping and weak damping limits [29],

$$\tau_0 \simeq \begin{cases} \frac{\pi\gamma}{\omega_0^2}e^{U_0/k_BT} & \text{for } \gamma \gg \omega_0, \\ \frac{\pi}{4\gamma}\frac{k_BT}{U_0}e^{U_0/k_BT} & \text{for } \gamma \ll \omega_0, \end{cases} \tag{5}$$

where $\omega_0 = 2\pi\sqrt{2U_0/(mL^2)}$ is the curvature of the potential at the bottom of the well. Both expressions are valid in the limit of deep potentials $U_0 \gg k_BT$. This timescale is exponential in the potential depth and increases as either the high- or low-dissipation limit is approached. We note that more involved formulas that provide a better approximation for moderately deep potentials may also be obtained [30].

For strong damping, the particle immediately equilibrates after escaping to a neighboring well and thus the probability of jumping multiple lattice sites is negligible [28]. In this limit, the jump length distribution is simply $\phi(\xi) = \delta(\xi \pm L)/2$. By contrast, in the weak damping regime, once the particle attains an energy sufficient for escaping, the relaxation of the energy back towards the

thermal average is slow, and the particle can jump over multiple wells before becoming trapped again. An expression for the jump-length distribution, valid at low dissipation, may be obtained from the discrete probability $\phi^*(n)$ of jumping n lattice sites of the periodic potential in either direction derived by Mel'nikov [32],

$$\phi^*(n) = N\mathcal{P}\left(\frac{\mathcal{E}}{k_B T}n\right)$$
$$\text{with} \quad \mathcal{P}(y) = e^{-y/4}\int_0^\infty dz \frac{z^2 e^{-yz^2/4}}{(1+\sqrt{2+z^2})^2}, \qquad (6)$$

where N is a normalization constant such that $\sum_{n=1}^{\infty}\phi^*(n) = 1$. The continuous jump-length distribution follows as $\phi(\xi) = \phi^*(n)\delta(|\xi| - nL)$. The quantity $\mathcal{E}$ in Eq. (6) denotes the energy dissipated by a particle traveling a distance L at an energy U_0 that is just sufficient to escape from a well. It is given by [32],

$$\mathcal{E} = \sqrt{m}\gamma\int_0^L dx\sqrt{2[U_0 - U(x)]}. \qquad (7)$$

For the cosine-shaped potential, the integral Eq. (7) can be evaluated explicitly and yields $\mathcal{E} = 2\gamma L\sqrt{2mU_0}/\pi$. It is important to note that the function $\mathcal{P}(y)$ behaves as $\mathcal{P}(y) \propto y^{-1/2}$ for small y and as $\mathcal{P}(y) \propto y^{-3/2}e^{-y/4}$ for large y. The tails of the jump-length distribution are hence not exactly exponential. Contrary to a Lévy walk [21], the jumps are at least 2 orders of magnitude shorter than the waiting time for $U_0 \gtrsim 4k_B T$, even in the underdamped limit, and thus almost instantaneous.

Because of the exponential waiting-time distribution, Eq. (3), the CTRW is memoryless. The n-point probability distributions hence factorize [6,7]. The 2-point probability density can, for example, be written as the product,

$$P(x_2, t_2; x_1, t_1) = P(x_2 - x_1, t_2 - t_1)P(x_1, t_1). \qquad (8)$$

We can accordingly express arbitrary n-point correlation functions in terms of the characteristic function $K(k,t)$ using Eq. (4) [30]. The position 2-point correlation function is, for instance, given by

$$\langle x(t_2)x(t_1)\rangle = -\partial_k[K(k, t_2 - t_1)\partial_k K(k, t_1)]|_{k=0},$$
$$= -\frac{t_1}{\tau}\partial_k^2\hat{\phi}(k)|_{k=0} = \frac{t_1}{\tau}\langle\xi^2\rangle. \qquad (9)$$

In addition, the second and fourth moments read

$$\langle\Delta x^2(t)\rangle = \frac{t}{\tau_0}\langle\xi^2\rangle, \qquad (10)$$

$$\langle\Delta x^4(t)\rangle = \frac{t^2}{\tau_0^2}\left(3\langle\xi^2\rangle^2 + \frac{\tau_0}{t}\langle\xi^4\rangle\right), \qquad (11)$$

where we have defined the displacement $\Delta x(t) = x(t) - x(0)$. The second moment [Eq. (10)] is linear in time indicating that the position of the particle exhibits normal diffusion with diffusion coefficient $D_x = \langle\xi^2\rangle/(2\tau_0)$ at all times, as in the asymptotic Gaussian diffusion limit [19,20]. By contrast, the displacement distribution is not Gaussian at finite times. The departure from Gaussianity may be quantified with the excess kurtosis [19,20],

$$\kappa(t) = \frac{\langle\Delta x^4(t)\rangle}{3\langle\Delta x^2(t)\rangle^2} - 1 = \frac{\langle\xi^4\rangle}{3\langle\xi^2\rangle^2}\frac{\tau_0}{t}. \qquad (12)$$

This quantity is zero for Gaussian distributions. It is positive for the CTRW indicating that large displacements are more prevalent than in the Brownian case. The Gaussian limit is recovered for large times as $1/t$ with a rate that is controlled by the excess kurtosis of the step-size distribution, $\kappa_\xi = \langle\xi^4\rangle/(3\langle\xi^2\rangle^2)$. Because of the algebraic decay, deviations from Gaussian diffusion can be significant even at longs times.

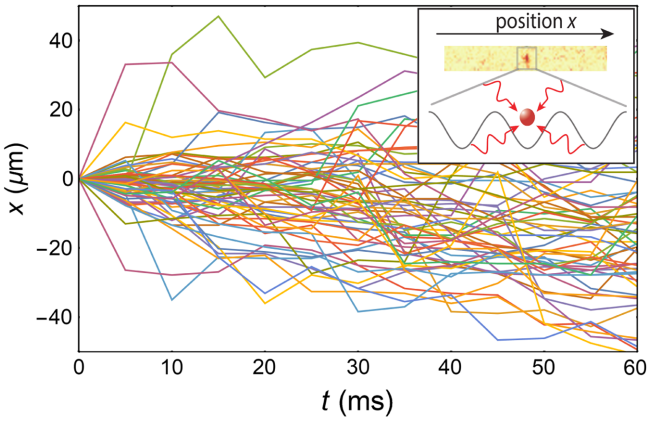

FIG. 1. Position of single cesium atoms diffusing in a 1D optical lattice as a function of time. The lines show 60 randomly chosen coarse-grained traces for a time between stroboscopic position measurements of $\tau_{\text{flight}} = 5$ ms. Inset: Sketch of the experiment. The atom moves in a periodic potential while interacting with the light field of the cooling laser. The imaging yields pictures as shown near the top of the inset with the red spot indicating the current position of the atom.

Single atoms in an optical lattice.—Our CTRW model Eq. (4) holds for any deep periodic potential, both in the underdamped and overdamped limits [30]. In order to test its predictions and determine its range of validity, we now apply it to experimental data obtained by measuring the motion of single atoms in an optical lattice [33]. In the experiment, a cesium atom is trapped in the periodic potential of a one-dimensional optical lattice with $U_0/k_B \approx 210\ \mu$K and $L = \lambda/2$ where $\lambda = 790$ nm is the wavelength of the lattice beam. Damping at a rate of $\gamma \approx 5 \times 10^3\ \text{s}^{-1}$ is due to a Doppler cooling force and noise is induced by random absorption and emission of photons, resulting in a recoil of the atom [26]. Both provide an effective thermal bath at a temperature of $T \approx 50\ \mu$K. The thermal energy is more than 4 times smaller than the lattice depth, corresponding to the deep-potential limit. Quantum tunneling is

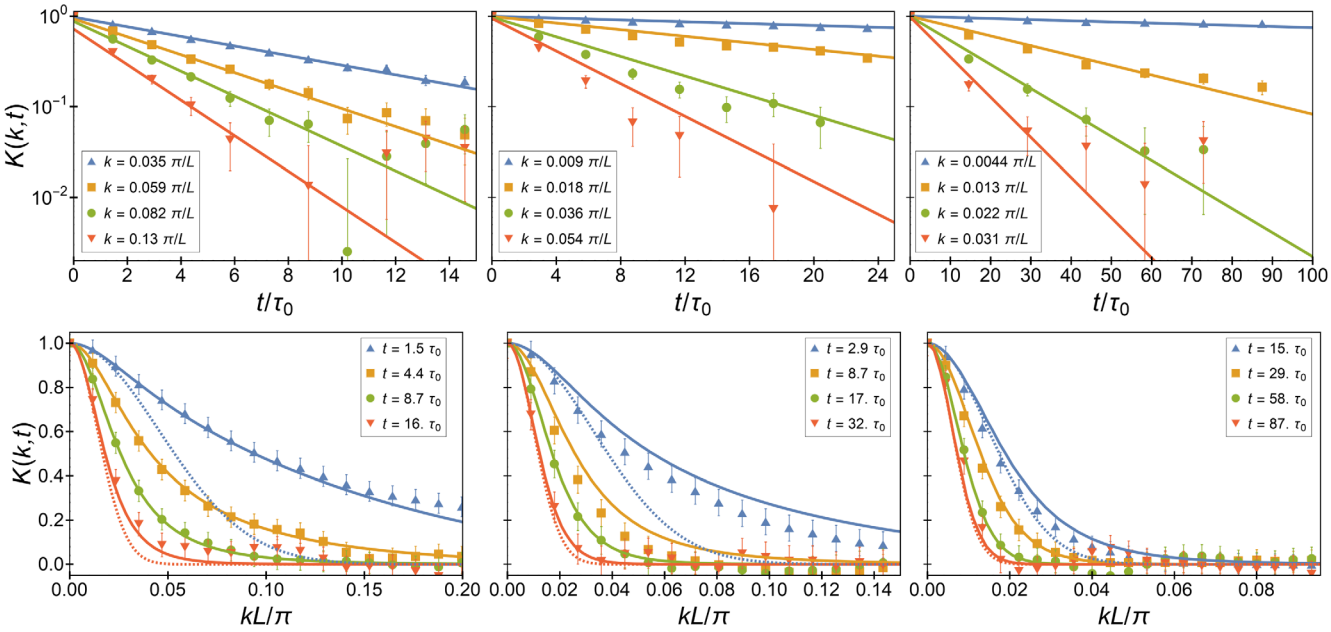

FIG. 2. Real part of the characteristic function $K(k,t)$ of single cesium atoms diffusing in a one-dimensional optical lattice as a function of time t (top) and wave vector k (bottom). The symbols correspond to the experimental data, the solid lines to the analytical prediction Eq. (4) with Eq. (6), evaluated using the experimental parameters $\mathcal{E} = 0.13 k_B T$ and $\tau_0 = 3.4$ ms, without any free parameter. The first, second, and third column correspond to $\tau_{\text{flight}} = 5$ ms, 10 ms, 50 ms, respectively. We observe very good agreement between data and theoretical predictions, in particular for small values of k, which reflect the long-range behavior of the jump process. From the panels in the top row, we see that the time dependence of the characteristic function at fixed k is well described by an exponential decay, confirming the validity of the exponential waiting time distribution, Eq. (3). On the other hand, the panels in the bottom row show that also the predicted dependence on k resulting from the jump length distribution [Eq. (6)] is well reproduced in the experiment. It further provides a much better description of the data than the asymptotic Gaussian diffusion approximation with the same diffusion coefficient (dashed lines), in particular at short times (blue). The error bars indicate the standard deviation of $\mathrm{Re}(K)$ due to the finite number of trajectories used in its computation. Note that the theoretical curves have been adjusted to explicitly take into account the measurement accuracy [30].

suppressed by frequent photon scattering with rates in the MHz regime. The atomic motion can thus be treated classically.

The jump-length distribution [Eq. (6)] is entirely specified by the energy dissipation per period of the lattice [Eq. (7)] which is equal to $\mathcal{E} \approx 0.13 k_B T$ in the experiment. This value corresponds to the weak damping regime $\gamma \ll \omega_0$. On the other hand, the waiting-time distribution [Eq. (3)] is fully characterized by the escape time τ_0 from a potential well, which for the experimental parameters is given as $\tau_0 \approx 3.4$ ms [30]. This is the central relevant time scale for the motion of the atom in the optical lattice.

The position of the atom after a time τ_{flight} is measured by ramping up the potential to $U^* \approx 850\ \mu$K while the cooling beam is switched off, effectively immobilizing the atom, and taking a high-resolution fluorescence image. Subsequently, the potential is lowered to U_0, allowing the atom to move again for a time τ_{flight}. Repeating this procedure 14 times for every atom generates a coarse-grained measurement of the diffusion process. For each parameter set, 600 to 1000 atomic trajectories are recorded (typical examples are shown in Fig. 1). The longest traces spread over approximately 100 lattice sites corresponding to a total distance of 40 μm. The position resolution is about 2 μm. A high number of photons (of the order of 10^6) are scattered during the image taking. The particle thus loses its memory about previous steps and jumps are independent of each other. From the experimental trajectories, we determine the characteristic function as $K(k,t) = \sum_{j=1}^{N} e^{ikx_j(t)}/N$, where $x_j(t)$ is the position of the atom in the jth measurement at time t. Compared to first computing the distribution $P(x,t)$ and then taking its Fourier transform, this method has the advantage of not requiring any spatial binning of the trajectory data, which inevitably introduces aliasing.

Figure 2 displays the real part of the characteristic function $K(k,t)$, both as a function of time t (top) and of the wave vector k (bottom) for increasing values of $\tau_{\text{flight}} = 5$ ms, 10 ms, and 50 ms. A small, nonzero imaginary part, which indicates a slightly asymmetrical position distribution, arises mainly as a consequence of the finite number of trajectories [30]. The symbols correspond to the experimental data and the lines to the analytical predictions given by Eq. (4) together with the jump-length distribution based on Eq. (6), evaluated using the experimental parameters

$\mathcal{E} = 0.13 k_B T$ and $\tau_0 = 3.4$ ms. We observe overall remarkable agreement between theory and experiment, without any free parameter. In particular, the t dependence of the characteristic function (left) confirms the exponential form of the waiting-time distribution [Eq. (3)], while the k dependence (right) corroborates the step-size distribution [Eq. (6)]. Deviations are seen for large values of k, that is, at short distances. These are, on the one hand, due to the finite spatial resolution of the imaging process and the determination of the system parameters that enter exponentially into the waiting time distribution. On the other hand, we note that, since the motion of the atoms is only weakly damped, the atoms do not immediately thermalize after a jump. Instead, they retain their energy on time scales of the energy autocorrelation time of $\tau_c = 0.24$ ms and thus have an increased probability to jump again. These repeated-jump events are not captured by the CTRW model. They cause the characteristic function to depart from Eq. (4) for values of $kL/\pi \gtrsim 1/\langle n \rangle \simeq 0.07$, where $\langle n \rangle \simeq 14$ is the average length of a single jump in the experiment [30]. Such deviations do not occur in the overdamped regime [30]. Comparing the CTRW of the atoms with standard Gaussian diffusion, the difference is clearly visible at short times (blue dashed lines in Fig. 2, in particular for the short flight time $\tau_{\text{flight}} = 5$ ms). By contrast, on time scales that are very long compared with the escape time τ_0, the position of the particle is the sum over many independent jump events, and the distribution converges towards a Gaussian in accordance with the central-limit theorem (red dashed lines).

Conclusions.—We have derived a continuous-time random walk model for a Brownian particle in a periodic potential. This model represents an intermediate level of coarse graining between the full microscopic dynamics and a simple diffusion approximation. As such, it permits a detailed, yet analytical characterization of the statistics of the process. It is valid for deep potentials, $U_0 \gtrsim 4 k_B T$, both in the underdamped and overdamped regimes. We have concretely determined the waiting-time and jump-length distributions, from which we have obtained the dynamical structure factor and the non-Gaussian characteristic function. We have, additionally, observed excellent agreement between theoretical predictions and experimental data for the weakly damped diffusion of single laser-cooled cesium atoms moving in a one-dimensional optical lattice, without any free parameter. Our results establish a transparent and useful bridge between microscopic and macroscopic theoretical descriptions of a paradigmatic nonequilibrium system and, at the same time, between analytical formulas and experiment.

This work was supported by the World Premier International Research Center Initiative (WPI), MEXT, Japan, by JSPS Grant-in-Aid for Scientific Research on Innovative Areas "Discrete Geometric Analysis for Materials Design": Grant No. 17H06460 and by Deutsche Forschungsgemeinschaft (DFG) via Sonderforschungsbereich (SFB) 49.

[1] B. Español, in *Statistical Mechanics of Coarse-Graining*, Lectures Notes in Physics Vol. 640 (Springer, Berlin, 2004), pp. 69–115.
[2] P. Castiglione, M. Falcioni, A. Lesne, and A. Vulpiani, *Chaos and Coarse Graining in Statistical Mechanics* (Cambridge University Press, Cambridge, England, 2008).
[3] P. Ehrenfest and T. Ehrenfest, *The Conceptual Foundation of the Statistical Approach in Mechanics* (Cornell University Press, New York, 1956).
[4] R. Jancel, *Foundations of Classical and Quantum Statistical Mechanics* (Pergamon Press, Oxford, 1963).
[5] R. Zwanzig, *Nonequilibrium Statistical Mechanics* (Oxford University Press, Oxford, 2001).
[6] B. D. Hughes, *Random Walks and Random Environments* (Clarendon Press, Oxford, 1996).
[7] J. Klafter and I. M. Sokolov, *First Steps in Random Walks* (Oxford University Press, Oxford, 2011).
[8] W. Hans and K. W. Kehr, Diffusion in regular and disordered lattices, Phys. Rep. **150**, 263 (1987).
[9] J.-P. Bouchaud and A. Georges, Anomalous diffusion in disordered media: Statistical mechanisms, models and physical applications, Phys. Rep. **195**, 127 (1990).
[10] R. Metzler and J. Klafter, The random walk's guide to anomalous diffusion: A fractional dynamics approach, Phys. Rep. **339**, 1 (2000).
[11] F. Höfling and T. Franosch, Anomalous transport in the crowded world of biological cells, Rep. Prog. Phys. **76**, 046602 (2013).
[12] V. Zaburdaev, S. Denisov, and J. Klafter, Lévy walks, Rev. Mod. Phys. **87**, 483 (2015).
[13] I. Wong, M. Gardel, D. Reichman, E. Weeks, M. Valentine, A. Bausch, and D. Weitz, Anomalous Diffusion Probes Microstructure Dynamics of Entangled F-Actin Networks, Phys. Rev. Lett. **92**, 178101 (2004).
[14] J.-H. Jeon, V. Tejedor, S. Burov, E. Barkai, C. Selhuber-Unkel, K. Berg-Srensen, L. Oddershede, and R. Metzler, In Vivo Anomalous Diffusion and Weak Ergodicity Breaking of Lipid Granules, Phys. Rev. Lett. **106**, 048103 (2011).
[15] A. V. Weigel, B. Simon, M. M. Tamkun, and D. Krapf, Ergodic and nonergodic processes coexist in the plasma membrane as observed by single-molecule tracking, Proc. Natl. Acad. Sci. U.S.A. **108**, 6438 (2011).
[16] S. Sadegh, E. Barkai, and D. Krapf, Five critical exponents describing $1/f$ noise for intermittent quantum dots, New J. Phys. **16**, 113054 (2014).
[17] J. Klafter and R. Silbey, Derivation of the Continuous-Time Random-Walk Equation, Phys. Rev. Lett. **44**, 55 (1980).
[18] D. A. Kessler and E. Barkai, Theory of Fractional Lévy Kinetics for Cold Atoms Diffusing in Optical Lattices, Phys. Rev. Lett. **108**, 230602 (2012).
[19] H. Risken, *The Fokker-Planck Equation* (Springer, Berlin, 1989).
[20] W. T. Coffey, Y. P. Kalmykov, and J. T. Waldron, *The Langevin Equation* (World Scientific, Singapore, 2004).

[21] J. M. Sancho, A. M. Lacasta, K. Lindenberg, I. M. Sokolov, and A. H. Romero, Diffusion on a Solid Surface: Anomalous is Normal, Phys. Rev. Lett. **92**, 250601 (2004).
[22] B. Wang, S. M. Anthony, S. C. Bae, and S. Granick, Anomalous yet Brownian, Proc. Natl. Acad. Sci. U.S.A. **106**, 15160 (2009).
[23] B. Wang, J. Kuo, S. C. Bae, and S. Granick, When Brownian diffusion is not Gaussian, Nat. Mater. **11**, 481 (2012).
[24] E. W. Montroll and G. H. Weiss, Random walks on lattices II, J. Math. Phys. (N.Y.) **6**, 167 (1965).
[25] G. Grynberg and C. Mennerat-Robilliard, Cold atoms in dissipative optical lattices, Phys. Rep. **355**, 335 (2001).
[26] H. J. Metcalf and P. van der Straten, *Laser Cooling and Trapping* (Springer, Berlin, 1999).
[27] E. Lutz and F. Renzoni, Beyond Boltzmann-Gibbs statistical mechanics in optical lattices, Nat. Phys. **9**, 615 (2013).
[28] R. Ferrando, R. Spadacini, and G. E. Tommei, Kramers problem in periodic potentials: Jump rate and jump lengths, Phys. Rev. E **48**, 2437 (1993).
[29] P. Hänggi, P. Talkner, and M. Borkovec, Reaction rate theory: Fifty years after Kramers, Rev. Mod. Phys. **62**, 251 (1990).
[30] See Supplemental Material at http://link.aps.org/supplemental/10.1103/PhysRevLett.123.070602 for escape rates in the overdamped and underdamped limit, higher-order correlation functions, comparison to numerical simulation and discussion of aliasing and measurement errors, which includes Ref. [31].
[31] E. T. Whittaker and G. N. Watson, *A Course in Modern Analysis* (Cambridge University Press, Cambridge, England, 1990).
[32] V. I. Mel'nikov, The Kramers problem: Fifty years of developments, Phys. Rep. **209**, 1 (1991).
[33] F. Kindermann, A. Dechant, M. Hohmann, T. Lausch, D. Mayer, F. Schmidt, E. Lutz, and A. Widera, Nonergodic diffusion of single atoms in a periodic potential, Nat. Phys. **13**, 137 (2017).